Effects of Propeller Pitch and Number of Blades on Energy Saving of an ECO-Cap

MARINE 2021

Yosuke Kobayshi[1,*], Yoshihisa Okada[1], Kenta Katayama[1],

Takamichi Hiroi[2], Daisuke Wako[2], and Yasuo Ichinose[2]

[1] Nakashima Propeller Co., Ltd., 688-1, Joto-Kitagata, Higashi-ku, Okayama 709-0625, Japan.
Email: y-kobayashi@nakashima.co.jp, yoshihisa@nakashima.co.jp, ken-katayama@nakashima.co.jp,
web: https://www.nakashima.co.jp/

[2] National Maritime Research Institute, 6-38-1, Shinkawa, Mitaka, Tokyo, 181-0004, Japan.
Email: hiroi@m.mpat.go.jp, wako@m.mpat.go.jp, ichinose@m.mpat.go.jp ,
web: https://www.nmri.go.jp/

[*] Corresponding author: Yosuke Kobayashi, y-kobayashi@nakashima.co.jp

ABSTRACT

Propeller hub cap with fins (HCWF) is an energy-saving device, which is easily installed and replaced on ships in comparison with the other energy saving devices. Nakashima Propeller has developed a HCWF named ECO-Cap. This study discusses relations between energy-saving effects, propeller geometries, and flow fields behind the propellers based on propeller open water tests and underwater stereoscopic particle image velocimetry measurements in a towing tank using models of an ECO-Cap and multiple propellers. The test results showed that the ECO-Cap can suppress hub vortices and improve propulsion efficiency up to 4.7%. The propeller which has less number of blades or root-loaded pitch distribution strengthened hub vortices during a normal cap without fins. The intensity of the hub vortices was different during the normal cap between the propellers but almost the same level regardless of the propellers during the ECO-Cap. The results suggest that potential energy-saving amount by the ECO-Cap largely depends on the intensity of the hub vortices during the normal cap. Including the energy-saving effects of the ECO-Cap into the propeller open water efficiency, ranking of the propulsion efficiency changed from the original propeller open water efficiency without the ECO-Cap. The results showed importance of designing propellers and HCWFs considering interaction between components.

Keywords: Propeller, ECO-Cap, Propeller hub cap with fins (HCWF), Energy saving device (ESD), Stereoscopic particle image velocimetry (SPIV) measurement.

NOMENCLATURE

D_P	Propeller diameter [m]
$C_{0.7R}$	Blade chord length at 0.7R [m]
T	Thrust [N]
Q	Torque [N m]
w	Wake factor [-]
ρ	Density of water [kg m^{-3}]
ν	Kinematic viscosity [m^2 s^{-1}]
V_S	Ship speed [m s^{-1}]

1. INTRODUCTION

With IMO's strategy to reduce greenhouse gas (GHG) emission, GHG reductions are required for not only newbuilding ships but also existing ships. Energy Efficiency Design Index (EEDI) is a technical measure of newbuilding ship, assuring that ship designs achieve a certain level of efficiency and decrease carbon emissions. For both newbuilding and existing ships, Energy Efficiency Existing Ship Index (EEXI) regulation and Carbon Intensity Indicator (CII) rating system are supposed to start from 2023 to promote GHG reductions further. These regulations are mandatory for ocean-going ships and become more tightening gradually. To comply with such environmental regulations, there are growing demands for improving propulsion efficiency of ships.

Propeller hub cap with fins (HCWF) is an energy-saving device (ESD), which is easily installed and replaced on ships in comparison with the other ESDs. Propeller Boss Cap Fins (PBCF) is the most famous HCWF developed by Ouchi *et al.* (1988). Nakashima Propeller has developed a HCWF named ECO-Cap (Okada *et al.* 2013; Katayama *et al.* 2015; Okazaki *et al.* 2015). The profiles of ECO-Caps are shown in Figures 1 and 2. Besides them, there are many types of HCWFs in a market. In general, such HCWFs reduce propeller hub vortices for saving energy. Its energy-saving effect depends on its own shape, inflow wake to the propeller plane, propeller geometry, and the Reynolds number (Kawamura *et al.* 2013; Okazaki *et al.* 2015; Müller 2017; Kimura *et al.* 2018). Yet relation between energy-saving effects of ECO-Cap, propeller geometries, and flow fields behind propellers remains to be investigated enough.

In this paper, propeller open water tests (POTs) and underwater stereoscopic particle image velocimetry (SPIV) measurements were carried out in a towing tank by using models of an ECO-Cap and multiple propellers to investigate the relation between the energy-saving effects, the propeller geometries, and the flow fields behind the propellers.

Figure 1. ECO-Cap

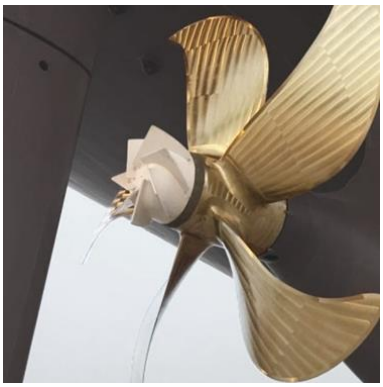

Figure 2. ECO-Cap installed on a propeller

2. MODEL TESTS SETUP

2.1 Models of propellers and caps

Four propeller models of different design in pitch distribution (root-loaded, constant, and tip-loaded) and in number of blades (four and five blades) were used as shown in Table 1 and Figure 3. The all propellers have the same non-dimensional chord length distribution and expanded area ratio. In order to avoid matching deviation of the propeller rotational speed between the propellers as possible, the pitch ratio was adjusted to be the same torque coefficient at a design stage. A normal cap without fins was used for comparison to confirm the effect of an ECO-Cap. The cap models shown in Figure 4 were used for Reverse POT condition.

Table 1. Propeller main particulars

Propeller model No.	P01	P02	P03	P04
Number of blades	4	4	4	5
Propeller diameter D_P [m]	0.2200	0.2200	0.2200	0.2200
Pitch ratio (0.7R)	0.6294	0.6500	0.6422	0.6363
Expanded area ratio	0.5500	0.5500	0.5500	0.5500
Hub ratio	0.1600	0.1600	0.1600	0.1600
Turning direction	Right	Right	Right	Right
Pitch distribution	Root loaded	Constant	Tip loaded	Constant

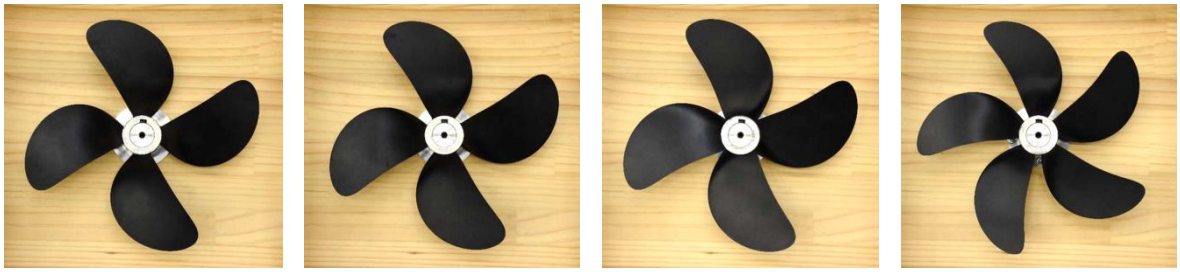

P01 P02 P03 P04

Figure 3. Propeller models

Normal cap ECO-Cap

Figure 4. Cap models

2.2 Propeller open water tests (POTs)

POTs were carried out in Normal POT and Reverse POT condition to confirm propeller open water characteristics and energy-saving effects by the combination of the propellers and the ECO-Cap. The test arrangements of the POTs are shown in Figure 5. The POTs were carried out at a towing tank of National Maritime Research Institute (NMRI). Wave suppress plate was used during Reverse POTs as shown in Figure 6 for preventing wave effect due to POT device. The test conditions were set as Kempf's Reynolds number R_{nK} = 6.0 × 10^5, where propeller advance coefficient J = 0. Propeller advance speed V_a, the Kempf's Reynolds number R_{nK}, and propeller advance coefficient J can be obtained from the following equations.

$$V_a = V_s(1 - w), \#(1)$$

$$J = \frac{V_a}{nD_P}, \#(2)$$

$$R_{nK} = \frac{C_{0.7R}\sqrt{{V_a}^2 + (0.7\pi nD_P)^2}}{\nu}, \#(3)$$

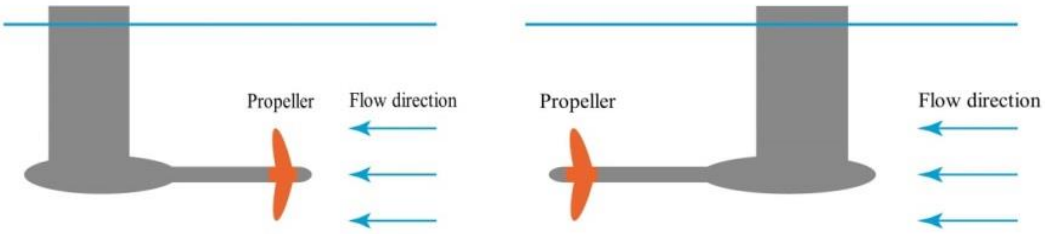

Normal POT Reverse POT

Figure 5. Normal POT and Reverse POT condition

Figure 6. Wave suppress plate for Reverse POT

Measurement range of J was set as covering assumed design point. The wake factor w was considered as 0 here for Normal POTs and Reverse POTs.

2.3 Stereoscopic particle image velocimetry (SPIV) measurements

SPIV measurements were carried out in Reverse POT condition to confirm the flow fields behind the propellers. The SPIV measurements were carried out at a towing tank of NMRI. SPIV measurement device is able to measure three components velocities at a certain plane by two CMOS cameras and double pulse laser. The arrangements of the SPIV measurements are shown in Figures 7 and 8. Averaged flow fields were obtained through statistical analysis from about 400 pairs of images captured during a run for the propellers P01, P02, and P03, and about 350 pairs of images for the propeller P04. The image acquisition interval was synchronized with a rotational angle of the propeller blade at a top position. Coordinate systems are shown in Figure 9. Propeller plane is positioned at X =0 in axial direction. The test conditions were set as $R_{nK} = 6.0 \times 10^5$ and J = 0.4. The J was selected as a near design point of the propellers. In order to avoid flooding the SPIV measurement device due to wave arise from higher towing speed, a draft of SPIV devise during P04 was set to be shallower than the draft of the other propellers.

Figure 7. SPIV measurement device

Figure 8. SPIV measurement of Reverse POT condition

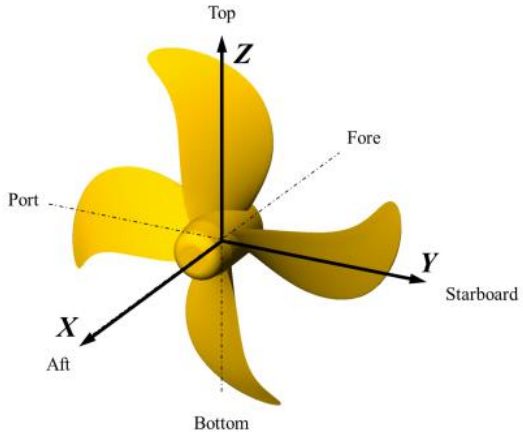

Figure 9. Coordinate systems

3. MODEL TEST RESULTS

3.1 Propeller open water characteristics

Thrust coefficient K_T, torque coefficient K_Q, and propeller open water efficiency η_O can be obtained from the measured thrust T, torque Q, towing speed V_s, and propeller rotational speed n through the following equations.

$$K_T = \frac{T}{\rho n^2 {D_P}^4}, \#(4)$$

$$K_Q = \frac{Q}{\rho n^2 {D_P}^5}, \#(5)$$

$$\eta_O = \frac{J K_T}{2\pi K_Q}, \#(6)$$

Normal POT results are shown in Figures 10 and 11. The highest η_O out of the four propellers was P04, followed in order by P02, P01, and P03. Compared with P01, P02 was 1.0% higher, P03 was 3.1% lower, and P04 was 3.0% higher propeller open water efficiency at a non-dimensional thrust load coefficient K_T/J^2 = 1.14 which is a representative design point of the propellers.

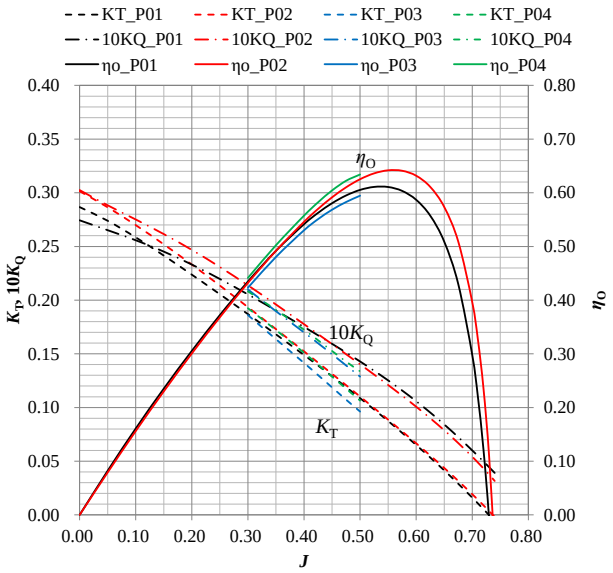

Figure 10. Propeller open water characteristics (J base)

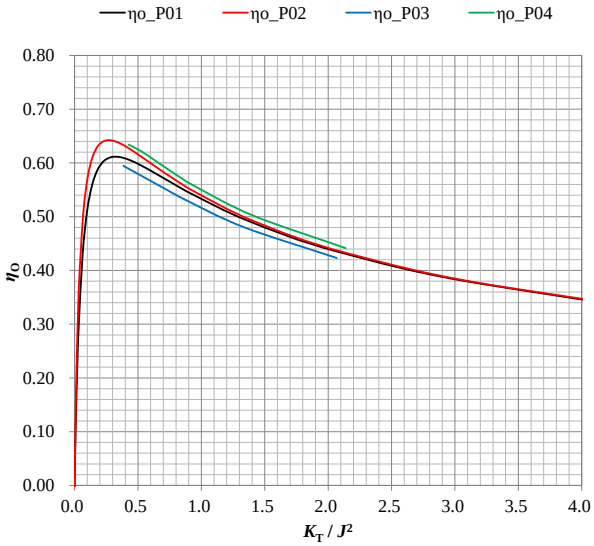

Figure 11. Propeller open water efficiency (K_T/J^2 base)

Reverse POT results are shown in Figures 12 and 13 as the rate of change from Normal cap to ECO-Cap of the propeller open water characteristics.The rate of change in K_T, K_Q, and η_O are calculated from following equations.

$$\Delta K_T = \frac{K_{T_{ecocap}}}{K_{T_{nomalcap}}} - 1, \#(7)$$

$$\Delta K_Q = \frac{K_{Q_{ecocap}}}{K_{Q_{nomalcap}}} - 1, \#(8)$$

$$\Delta \eta_O = \frac{\eta_{O_{ecocap}}}{\eta_{O_{nomalcap}}} - 1, \#(9)$$

In Figure 13, J = 0.4 was selected as a near design point of the propellers. The highest improvement in propeller open water efficiency by the ECO-Cap was confirmed for P01, followed in order by P02, P04. P03 has no significant improvement. For P01, P02, and P04, increase of K_T and decrease of K_Q resulted in the improvement of the propeller open water efficiency. P03 has no significant rate of change in K_T and K_Q. Comparing P02 with P04 focusing on difference in number of blades, decrease of K_Q was the same level but increase of K_T was larger for P02 which has less number of blades. These results lead to that less number of blades or root-loaded pitch is effective in improvement by the ECO-Cap. However, it is still debatable whether the improvement difference in number of blades comes from chord length or number of blades.

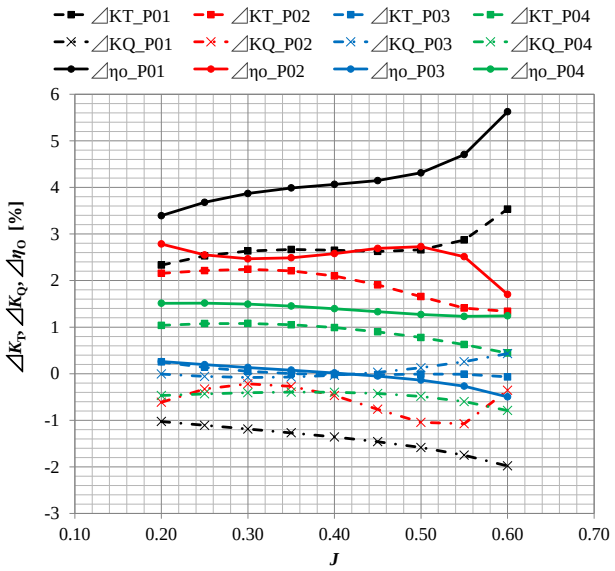

Figure 12. Effects on the propeller open water characteristics by the ECO-Cap

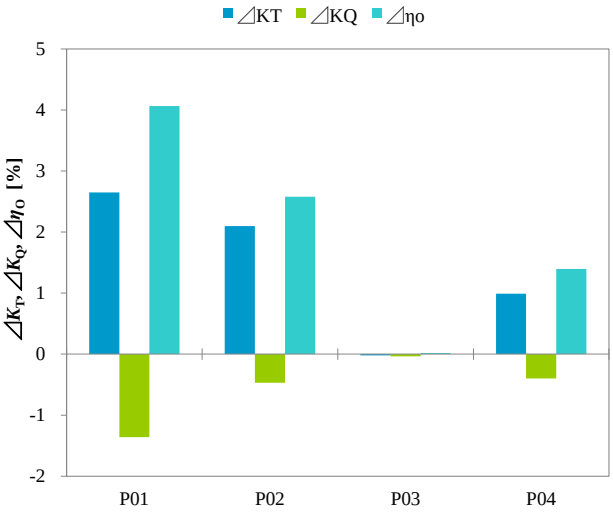

Figure 13. Effects on the propeller open water characteristics by the ECO-Cap at $J = 0.4$

For confirming the energy-saving effects, the improvement of the propeller open water efficiency by the ECO-Cap was arranged by thrust load coefficient K_T/J^2 as shown in the Figure 14 and compared at the same K_T/J^2 = 1.14 as shown in Figure 15. Energy-saving effects of the ECO-Cap were 4.7% for P01, 3.1% for P02, 0% for P03, and 1.7% for P04. Comparison of The propeller open water efficiency including energy-saving effects by the ECO-Cap at K_T/J^2 = 1.14 was shown in the Figure 16. Considering the ECO-Cap effects, the ranking of the propeller open water efficiency changed from the original propeller open water efficiency without the ECO-Cap. Including additional gains of the ECO-Cap, the highest propeller efficiency was P01 and almost the same as P04. Compared with P01, P02 was 0.5% lower, and P03 was 7.4% lower propulsion efficiency.

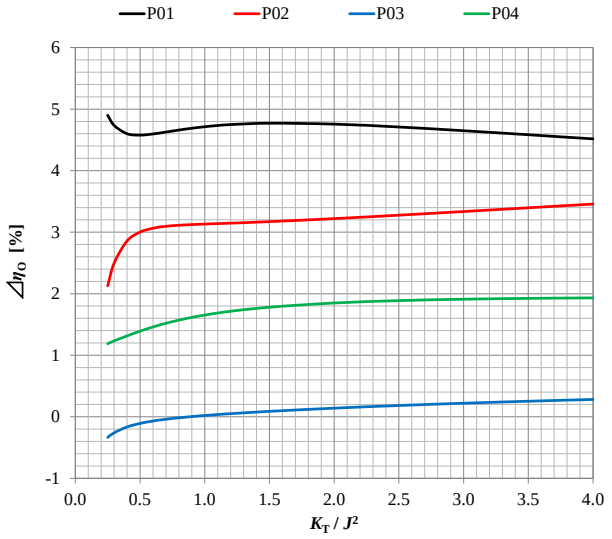

Figure 14. Effects on the propeller open water efficiency by the ECO-Cap (K_T/J^2 base)

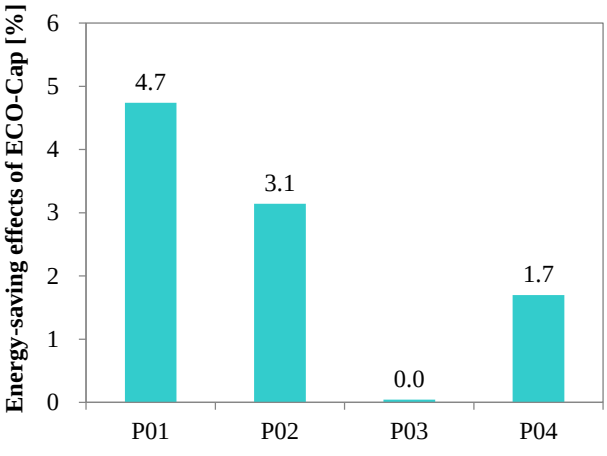

Figure 15. Energy-saving effects of the ECO-Cap at K_T/J^2 =1.14

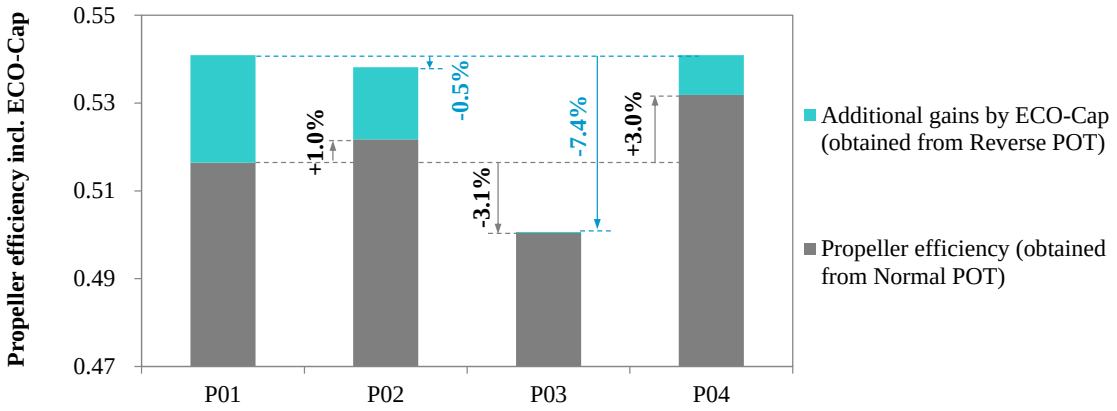

Figure 16. Comparison of the propeller efficiency including the ECO-Cap at $K_T/J^2 = 1.14$

3.2 Flow fields analysis

SPIV measurement results during Reverse POT condition are shown in Figures 17 to 24. Two circles in the figures mean the propeller diameter and the 70% radius position. Figure 17 shows the velocity distributions of P01 with the Normal cap and the ECO-Cap at a plane of $X = 0.1D_P$. Figures 18 and 19 show the velocity distributions of the four propellers with the Normal cap and the ECO-Cap at $X = 0.1D_P$ and $0.2D_P$. Figure 20 shows vorticity distributions, which show the magnitude of x-components of the vorticity, of P01 with the Normal cap and the ECO-Cap at a plane of $X = 0.1D_P$. Figures 21 and 22 show the vorticity distributions of the four propellers with Normal cap and ECO-Cap at $X = 0.1D_P$ and $0.2D_P$. The vorticity vector $\boldsymbol{\omega}$ is defined as:

$$\begin{aligned}\boldsymbol{\omega} &= (\omega_x, \omega_y, \omega_z) \\ &= \nabla \times \boldsymbol{v} \\ &= \left(\frac{\partial v_z}{\partial y} - \frac{\partial v_y}{\partial z}, \frac{\partial v_x}{\partial z} - \frac{\partial v_z}{\partial x}, \frac{\partial v_y}{\partial x} - \frac{\partial v_x}{\partial y}\right), \#(10)\end{aligned}$$

where, $\boldsymbol{v} = (v_x, v_y, v_z)$ means a vector of local flow velocity.

In Figures 17 and 20, the velocity and the vorticity distributions for P01 with Normal Cap show the strong vortex behind the propeller cap. The ECO-Cap shortened the velocity vector behind the propeller cap and weakened the vorticity behind the propeller cap. Thus, ECO-Cap can suppress the hub vortex. In Figures 18 and 21, the hub vortices during the Normal cap became stronger as the blade root pitch became larger, comparing the distributions with P01, P02, and P03 focusing on difference in propeller pitch. On the other hand, the intensity of the hub vortices during the ECO-Cap was almost the same level regardless of the propellers. The vorticity of P03, which was almost no improvement in propeller open water efficiency of the ECO-Cap, was almost the same level between the Normal cap and the ECO-Cap. Comparing P02 and P04, which have the same pitch distribution and different number of blades, the vorticity behind the propeller cap during the Normal cap was higher in P02 which improvement by the ECO-Cap was greater. Figures 19 and 22, which is more backward planes than that of Figures 18 and 20, shows similar tendencies to Figures 18 and 20 for the relation between the propellers, the Normal cap, and the ECO-Cap. Figures 23 and 24 show the principal velocity distributions and vector diagrams at $X = 0.3D_P$, $0.4D_P$ and $0.5D_P$. Focusing on the axial distance, the intensity of the hub vortices for the Normal cap and the ECO-Cap almost unchanged from $X = 0.1D_P$ to $0.5D_P$.

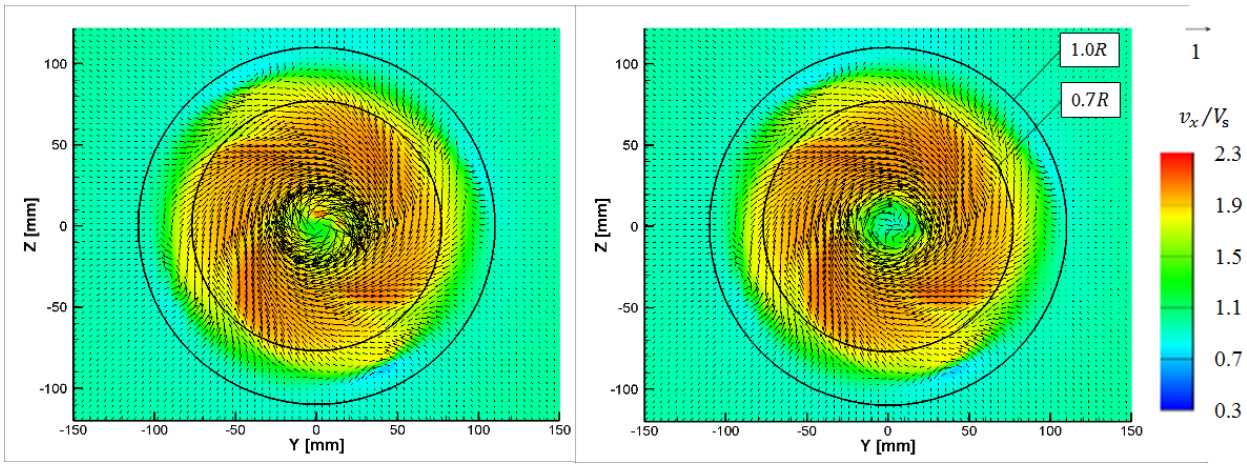

Normal cap ECO-Cap

Figure 17. Velocity distributions of P01 at a plane of $X = 0.1D_P$

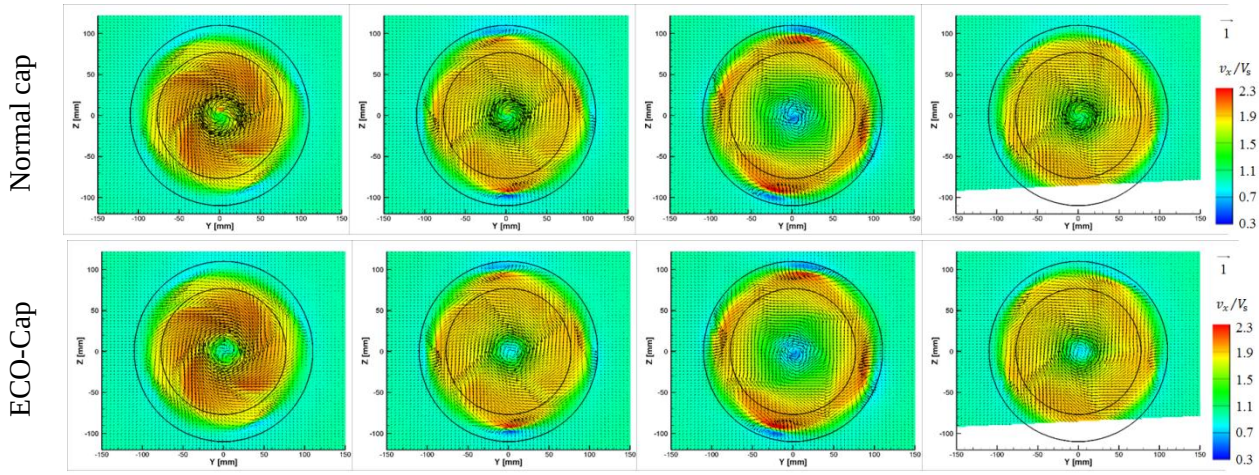

P01 P02 P03 P04

Figure 18. Velocity distributions of the propellers at $X = 0.1D_P$

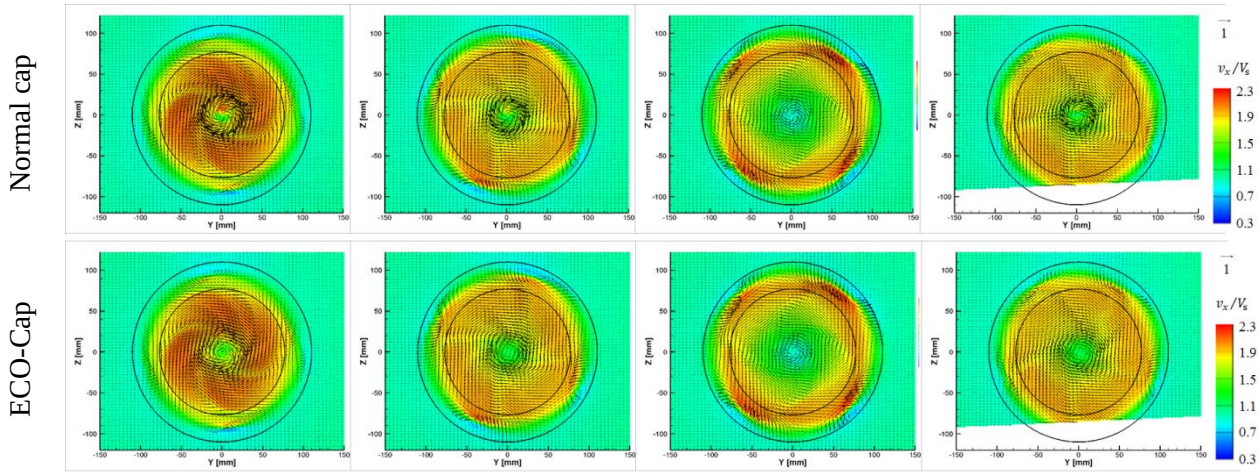

P01 P02 P03 P04

Figure 19. Velocity distributions of the propellers at $X = 0.2D_P$

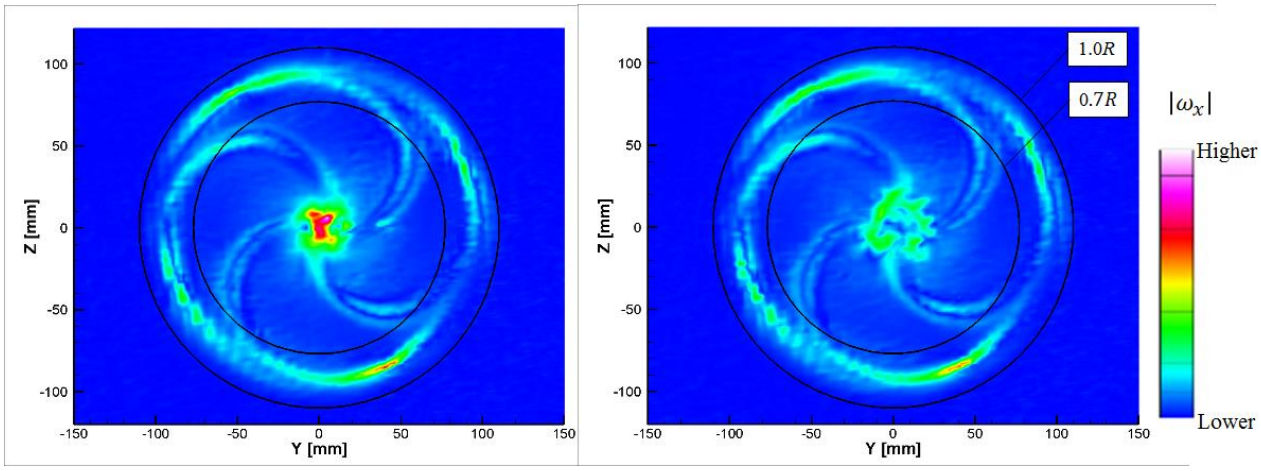

Figure 20. Vorticity distributions of P01 at a plane of $X = 0.1D_P$

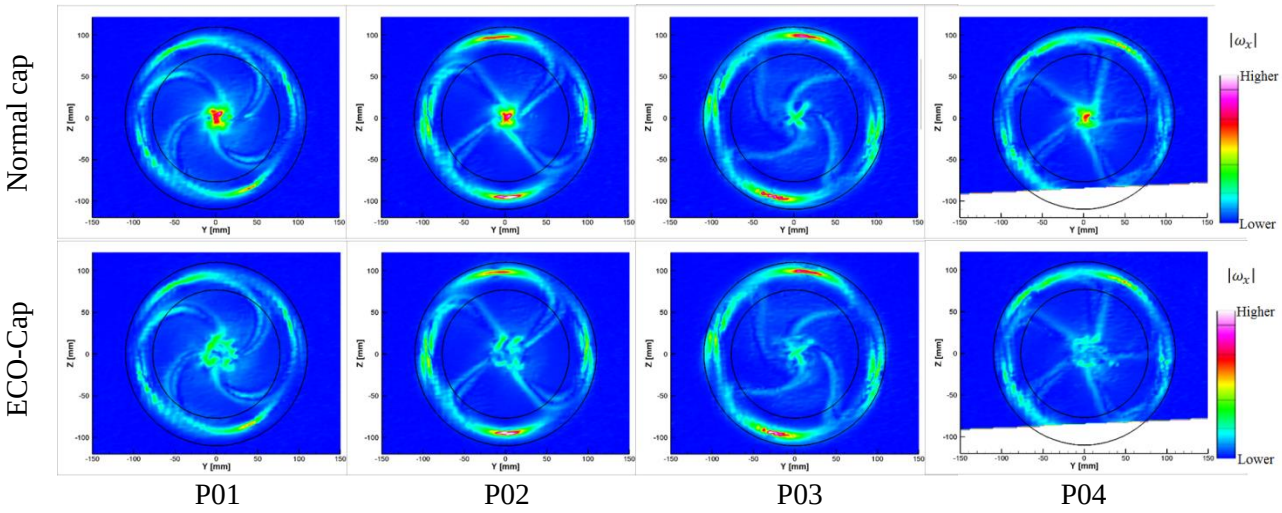

Figure 21. Vorticity distributions of the propellers at $X = 0.1D_P$

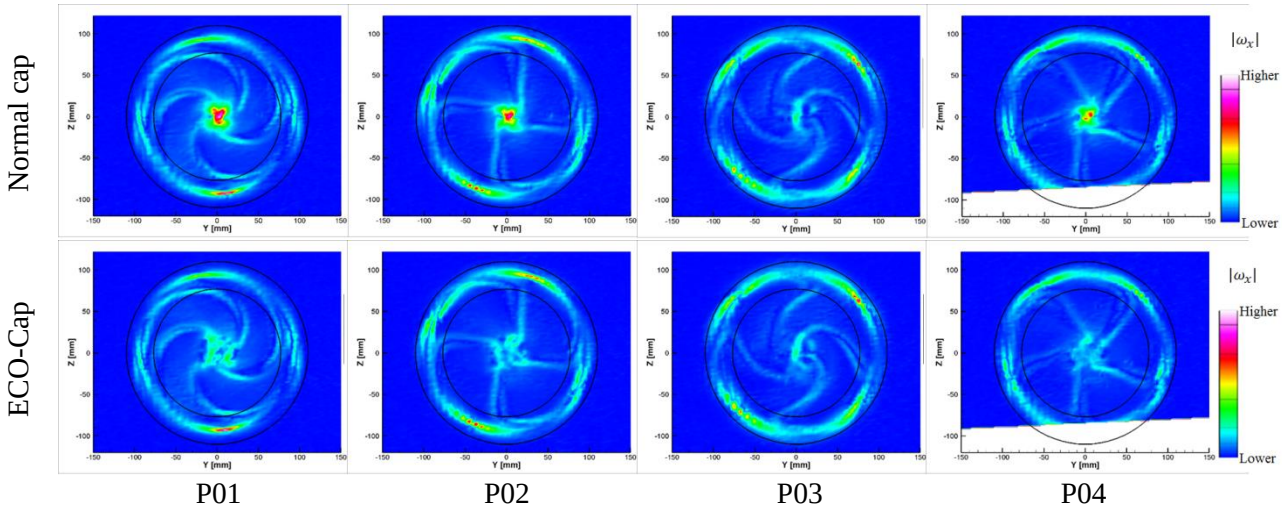

Figure 22. Vorticity distributions of the propellers at $X = 0.2D_P$

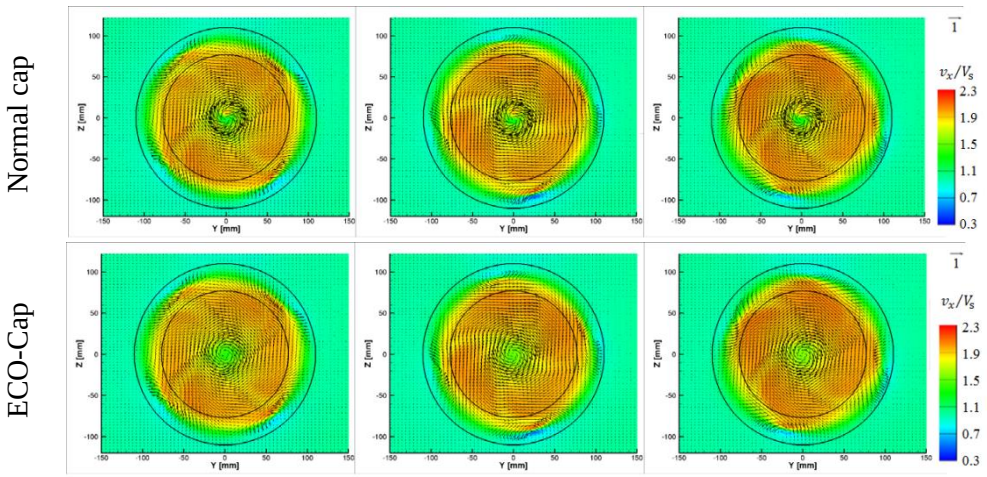

Figure 23. Velocity distributions of P02 behind the propeller plane

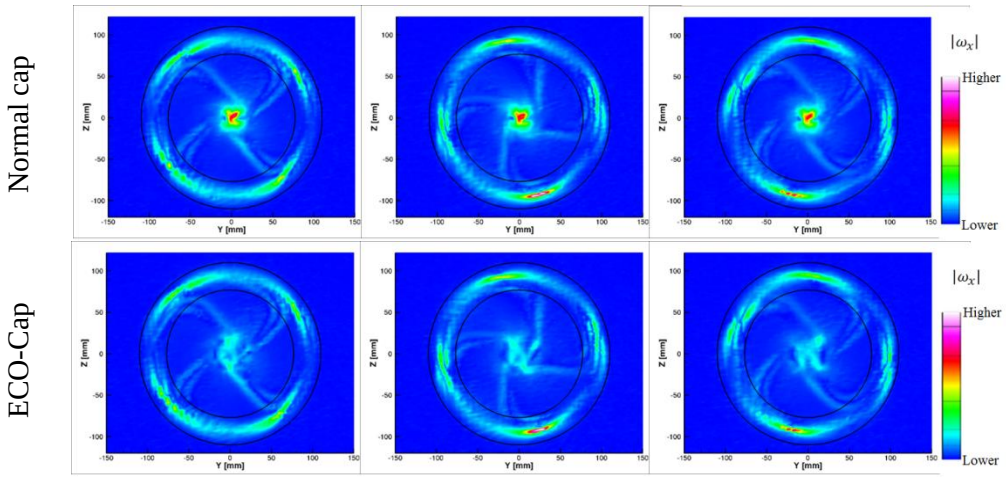

Figure 24. Vorticity distributions of P02 behind the propeller plane

4. CONCLUSIONS

The main objective of this paper is to investigate the relations between the energy-saving effects of the ECO-Cap and the propeller geometries through the flow fields behind the propellers. The results of POTs and SPIV measurements showed that the ECO-Cap can suppress hub vortices and improve propulsion efficiency up to 4.7%. The propellers which have less number of blades or root-loaded pitch distribution strengthen hub vortices behind the Normal cap. The intensity of the hub vortices was almost the same level regardless of the propellers during the ECO-Cap but different during the Normal cap between the propellers. The results suggest that potential energy-saving amount by the ECO-Cap largely depends on the intensity of the hub vortices during the normal cap. Including the energy-saving effects of the ECO-Cap into the propeller open water efficiency, the ranking of the propulsion efficiency changed from the original propeller open water efficiency without the ECO-Cap. The results showed importance of designing propellers and HCWFs considering interaction between components. Additionally, the interaction between the rudder, the other ESDs, and the hull during self-propulsion condition should be considered to achieve optimum design.

REFERENCES

Katayama, K., Okada, Y., and Okazaki, A. (2015), Optimization of the Propeller with ECO-Cap by CFD, Fourth International Symposium on Marine Propulsors smp'15, May 31-June 4, Austin, Texas, USA.

Kawamura, T., Ouchi, K., and Takeuchi, S. (2013), Model and full scale CFD analysis of propeller boss cap fins (PBCF), Third International Symposium on Marine Propulsors smp'13, May 5-8, Tasmania, Australia.

Kimura, K., Ando, S., Ono, S., Tanaka, Y., Takeuchi S., and Asanuma, N. (2018), Investigation on Full Scale Performance of the Propeller Boss Cap Fins (PBCF), Fill Scale Ship Performance, October 24-25, London, UK.

Müller, J. (2017),'HYTES' – HYKAT Tested Energy Saving Devises, The 5th International Conference on Advanced Model Measurement Technology for the Maritime Industry (AMT'17), October 11-13, Glasgow, UK.

Okada, Y., Okazaki, A., and Katayama, K. (2013), Numerical Analysis of the Propeller with Economical Cap by CFD, Proceedings of 16th Numerical Towing Tank Symposium, September 2-4, Mulheim, Germany.

Okazaki, M., Kajihama, T., Katayama, K., and Okada, Y. (2015), Propeller Particulars and Scale Effect Analysis of ECO-Cap by CFD, 18th Numerical Towing Tank Symposium, September 28-30, Cortona, Italy.

Ouchi, K., Ogura, M., Kono, Y., Orito, H., Shiotsu, T., Tamashima, M., and Koizuka, H. (1988), A Research and Development of PBCF (Propeller Boss Cap Fins) - Improvement of Flow from Propeller Boss -, Journal of the Society of Naval Architects of Japan, 163, 66-78.

Ouchi, K., Tamashima, M., Ogura, M., Kawasaki, T., and Koizuka, H. (1989), A Research and Development of PBCF (Propeller Boss Cap Fins) – 2nd Report: Study on Propeller Slipstream and Actual Ship Performance -, Journal of the Society of Naval Architects of Japan, 165, 43-53.

Ouchi, K. (1992), Effect and Application of PBCF (Propeller Boss Cao Fins), Journal of the Marine Engineering Society in Japan, Vol.27, No.9.

22nd ITTC, The Specialist Committee on Unconventional Propulsors, Final Report and Recommendations to the 22nd ITTC.